Electronic structure of α- and β-brass

R. S. Dhaka,[1] S. Banik,[1] A. K. Shukla,[1] V. Vyas,[2] Aparna Chakrabarti,[3] S. R. Barman,[1,*] B. L. Ahuja,[4] and B. K. Sharma[2]
[1]*UGC-DAE Consortium for Scientific Research, Khandwa Road, Indore 452001, India*
[2]*Department of Physics, University of Rajasthan, Jaipur, Rajasthan, 302015, India*
[3]*Raja Ramanna Centre for Advanced Technology, Indore 452013, India*
[4]*Department of Physics, M. L. Sukhadia University, Udaipur 313001, India*
(Received 13 March 2008; revised manuscript received 3 July 2008; published 25 August 2008)

The unoccupied conduction band and the occupied valence band of α- and β-brass (Cu-Zn) have been studied by inverse photoemission and photoemission spectroscopy. The experimental spectra have been interpreted with the help of calculations based on full potential linearized augmented plane wave method using density functional theory. The modification of the conduction and valence bands between α- and β-brass is related to the change in structure and increase in Zn content. For CuZn, the density of states exhibits a monotonic decrease across the Fermi level (E_F) with a dip at about 2 eV above E_F, but no evidence of a minimum representing a pseudogap is observed at E_F.

DOI: 10.1103/PhysRevB.78.073107 PACS number(s): 78.70.−g, 71.20.−b, 79.60.−i

Brass (Cu-Zn) has played an important role in the development of human civilization and is a classic system for fundamental research.[1–14] Brass with equal amount of Cu and Zn has a stable phase called β-brass. On the other hand, α-brass has a lower Zn content that can vary up to 30%. They are structurally different: α-brass is fcc while β-brass has an ordered CsCl type structure at room temperature. However, β-brass is bcc at high temperature with Cu and Zn atoms randomly arranged and becomes ordered upon cooling below about 450 °C. The structural difference is interesting because it shows that, starting from pure fcc Cu, replacement of about one half of the atoms by Zn that has only one electron more than Cu is sufficient to change the structure. CuZn is generally considered to be a Hume-Rothery alloy with valence electron to atom ratio of 1.5.[15,16]

Different theoretical studies exist in literature on the electronic structure of brass including the effect of disorder spanning several decades,[1–10] although some of the earlier works were not self-consistent.[7–10] While some earlier experimental works on Cu-Zn using x-ray photoemission spectroscopy (XPS) are available,[11–13] the unoccupied states above E_F have not been studied and no comparison between experiment and theory exists in literature. Here, we study the electronic structure of α- and β-brass using inverse photoemission spectroscopy (IPES) and XPS that directly probe the unoccupied conduction band and occupied valence band, respectively. The experimental spectra are interpreted by theoretical calculations based on full potential linearized augmented plane wave (FPLAPW) method.

α- and β-brass single-crystal specimens, grown along [110] direction, were obtained from Metal Crystals and Oxides Ltd., U.K. The purity of the sample is better than 99.99%. IPES measurements were performed in an ultrahigh vacuum (UHV) chamber with a base pressure of 6×10^{-11} mbar. An electrostatically focused electron gun of Stoffel Johnson design and an acetone gas filled photon detector with a CaF_2 window have been used.[17] IPES has been performed in the isochromat mode where the kinetic energy of the incident electrons has been varied at 0.05 eV steps and photons of fixed energy (9.9 eV) are detected with an overall resolution of 0.55 eV. The spectra are normalized by dividing the photon intensity by the current through the sample.[18] The samples were mechanically scraped using a diamond file to obtain an atomically clean surface in UHV. The absence of oxygen and carbon contamination was checked by recording O 1*s* and C 1*s* spectra that were in the noise level. In order to determine the surface compositions, the areas under the Cu 2*p* and Zn 2*p* have been determined by fitting the core-level peaks using a least square error minimization routine. From the analysis of the relative intensities of the Cu 2*p* and Zn 2*p*, considering their respective photoemission cross sections, the mean free path of the photoelectron and the analyzer transmission function,[19] the compositions of α- and β-brass turn out to be $Cu_{0.95}Zn_{0.05}$ and $Cu_{0.6}Zn_{0.4}$, respectively.

β-brass studied by us has CsCl structure that is ordered (as confirmed by x-ray diffraction) and the surface composition is $Cu_{0.6}Zn_{0.4}$. Thus, some of the Cu atoms (10% of the total number of atoms) occupy the Zn sites and this nonstoichiometry results in site disorder. α-brass is fcc with a composition of $Cu_{0.95}Zn_{0.05}$. Here, only 5% Zn atoms randomly replace the Cu atoms. Since the extent of disorder and nonstoichiometry in the brass samples studied here is small, the calculations have been performed for the ordered and stoichiometric CuZn and Cu. This approximation is justified by the good agreement between experiment and theory that we obtain (discussed later). Besides, theory is used to provide valuable input to the understanding of the nature of states. Compared to an ordered stoichiometric system, shift and broadening of the XPS peaks may occur due to nonstoichiometry and disorder.[11,12,14] However, different studies have shown that for the valence band, disorder generally broadens the spectral features.[2,21–24] The DOS calculated by Rowlands *et al.*[2] for ordered and disordered CuZn clearly show this.

The *ab initio*, relativistic FPLAPW calculations were performed with generalized gradient approximation[25] (GGA) for the exchange correlation using WIEN97 code.[26] An energy cutoff for the plane-wave expansion of 16 Ry is used ($R_{MT}K_{max}=9$). The maximum l (l_{max}) for the radial expansion was taken to be 10, and the maximum l for the nonspherical part ($l_{max,ns}$) was 4. The cutoff for charge density was $G_{max}=14$, as in our earlier work.[20] The muffin-tin radii

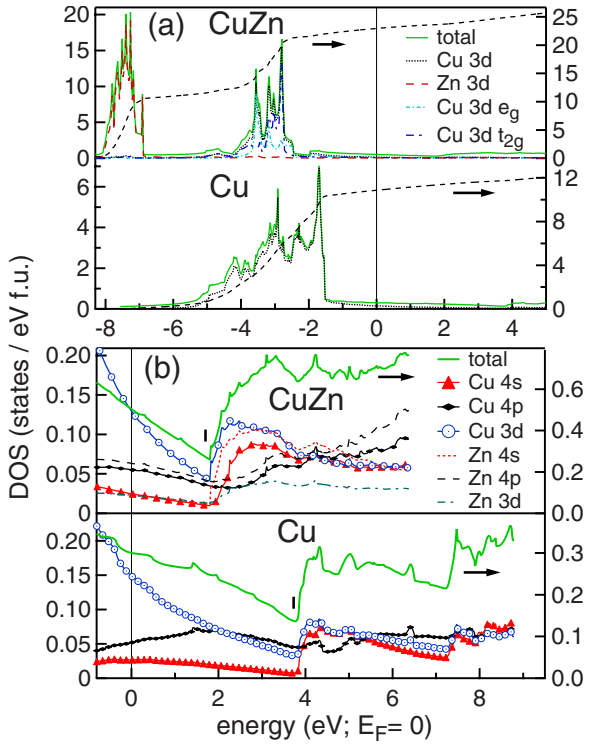

FIG. 1. (Color online) (a) The calculated density of states (DOS) and the partial DOS for CuZn compared with Cu metal. The dashed line shows integrated total DOS. (b) The unoccupied part of the DOS for CuZn and Cu shown in an expanded scale.

for both Cu and Zn are 2.4 a.u. The number of k points for self-consistent field cycles is taken to be 8000, resulting in 220 and 256 k points in the irreducible part of the Brillouin zone for CuZn and Cu, respectively. The energy and charge convergence were set at 0.1 mRy and 0.001 electronic charge, respectively. The lattice constant for the CsCl structure of CuZn is taken to be 5.5821 a.u.,[3] while copper is fcc with a=6.8219 a.u.

In the occupied part below the Fermi level (E_F=0 eV), the CuZn DOS is dominated by Cu 3d states centered around −3 eV, while the Zn 3d states appear as semicore states around −7.5 eV [Fig. 1(a)]. The Cu 3d t_{2g} states appear at higher energy with the most intense peak at −2.8 eV, while the e_g states are at lower energy with the highest peak at −3.6 eV. The contribution of the s and p states (not shown in [Fig. 1(a)]) is negligible compared to the d states over the entire range. For Cu metal, the Cu 3d states are centered around −2.5 eV, and the width of the valence band extends from −1.5 to −5 eV and the 3d band edge is shifted toward E_F compared to CuZn. Also the 3d bandwidth of Cu is larger than that of CuZn, which might be related to larger overlap of the 3d levels in close-packed fcc Cu, compared to CuZn with CsCl structure. The Cu-Cu distance in Cu is 4.82 a.u., while in CuZn it is 5.58 a.u. For CuZn (Cu), the integrated DOS at E_F is 23 (11) [Fig. 1(a)]. From our calculation, the charges corresponding to Cu and Zn are 11.1 and 11.9, respectively. This indicates a small charge transfer from Zn to Cu in CuZn, in agreement with earlier work.[6]

The unoccupied DOS of CuZn is much smaller in intensity compared to the occupied states and is shown in an expanded scale in Fig. 1(b). At E_F, no minimum indicative of a pseudogap is observed in the total DOS (and the partial DOS); rather the DOS decreases monotonically across E_F and exhibits a dip around 2 eV (shown by tick). Occurrence of a minimum at E_F was also not reported in earlier studies for both ordered and disordered CuZn.[2,6,7] Absence of clear pseudogap in CuZn may be related to the absence of s, p-d hybridization, unlike in Al-Mn and related alloys.[27] The DOS between 0 to 2 eV has predominant contributions from Cu 4p, Zn 4p, and Cu 3d states. The increase in DOS above 2 eV is related to Cu 4s, Zn 4s, and Cu 3d states. The Zn 3d states hardly contribute in the unoccupied region, which is understandable because of the fully filled $3d^{10}$ configuration of Zn. On the other hand, Cu has $3d^9$ configuration with one hole that would add intensity to the unoccupied states. Thus, while Cu 3d is dominant both below and above 2 eV, the 4p (4s) states are predominant below (above) 2 eV. For Cu metal, the minimum in the DOS appears at about 4 eV and the main contribution comes from the Cu 3d states.

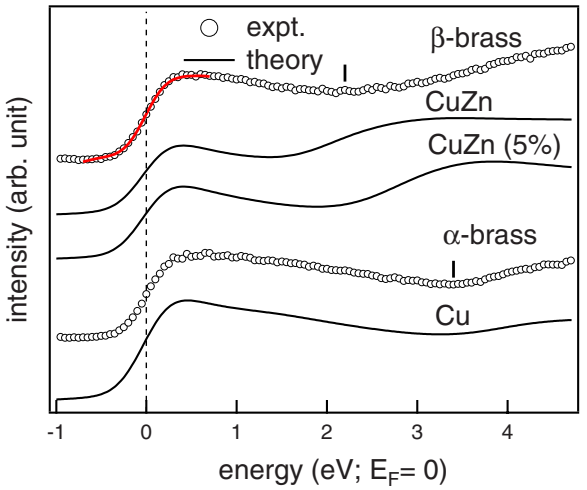

FIG. 2. (Color online) Experimental inverse photoemission spectra of α-brass and β-brass compared with calculated spectra for Cu, CuZn, and CuZn with 5% lattice contraction. The solid red curve through the experimental data of β-brass is obtained by least square fitting (see text). The spectra are staggered along the vertical axis.

In Fig. 2, the experimental IPES spectra of α- and β-brass are shown. Both spectra exhibit a smooth nearly free-electron-like parabolic shape up to 3.4 and 2.2 eV for α- and β-brass (shown by tick), respectively. Above this minimum, the spectral intensity increases. A good fit to the Fermi edge can be obtained by taking a constant DOS multiplied by the Fermi function that is convoluted with the instrumental resolution (solid red line in Fig. 2). This indicates absence of pseudogap in β-brass. However, if the width of the pseudogap around E_F is small (20–30 meV), it might be masked by the scatter in the experimental data and so its possible occurrence cannot be completely ruled out from the experimental spectrum.

The conduction bands have been calculated by broadening the unoccupied total DOS in Fig. 1(b) by the instrumental resolution. Besides, an energy dependent lifetime broadening has been used, represented by a Lorentzian with the

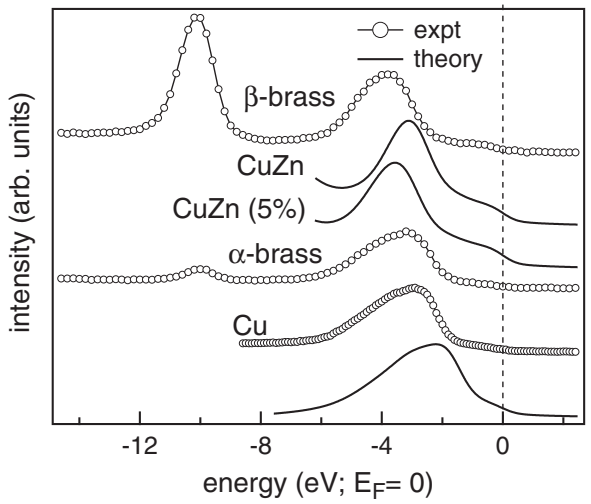

FIG. 3. Valence band spectra of α-brass, β-brass, and Cu metal compared with the calculated spectra for Cu, CuZn, and CuZn with 5% lattice contraction.

full width at half maximum (FWHM) of $0.3E$, where E is the energy with respect to E_F.[22,23,28] The calculated spectra are in fairly good agreement with experiment (Fig. 2). Thus, both experiment and theory show that the Cu p, d-Zn p dominated parabolic band becomes narrower in β-brass. The reasons for this are discussed later.

The XPS valence band spectra of β-brass, α-brass, and Cu are compared with the calculated valence band spectra (Fig. 3). The valence band spectra are calculated by broadening the occupied DOS (as discussed above) of CuZn and Cu [Fig. 1(a)]. The XPS valence band of β-brass exhibits two almost symmetric peaks at -3.8 and -10.1 eV, which can be identified as Cu $3d$ and Zn $3d$, respectively, by comparing with Fig. 1(a). The Zn $3d$ peak being more localized has smaller FWHM compared to the Cu $3d$ peak. The shape of the calculated valence band shows good agreement with experiment, and the partial contributions show that -3.8 eV peak is indeed Cu $3d$ related, while the low intensity states between -2 eV and E_F has sizable contributions from the Cu $3d$ e_g states. For α-brass, the Cu $3d$ peak is shifted toward lower binding energy (BE), i.e., toward E_F by 1 eV compared to β-brass. It is clearly asymmetric and the FWHM is somewhat higher than β-brass, in agreement with the calculated valence band. The shape and position of the $3d$ peak in α-brass is very similar to Cu valence band spectrum, where an asymmetric $3d$ peak is observed around -3 eV (Fig. 3). The peak at -10 eV due to Zn $3d$ states is drastically reduced in intensity because of smaller Zn content. However, there is no shift of the Zn $3d$ peak between α- and β-brass.

To understand the change in α- and β-brass valence bands, we note that higher Zn concentration in β-brass increases the number of conduction electron to atom ratio. This, in a rigid-band model, would shift the E_F to higher energies. In the experiment, which is referred to E_F, this would cause a constant shift of all the levels to lower energies. However, since Zn $3d$ related peak does not exhibit any shift between α- and β-brass, this explanation based on rigid-band model is not tenable. Rather, in β-brass, increase in Zn content results in change of structure. This increases the average nearest-neighbor distance between Cu atoms and reduces the overlap between the Cu $3d$ states. Thus, narrowing and shift of the Cu $3d$ dominated unoccupied and occupied spectral shapes occur in β-brass (Figs. 2 and 3). This is in good agreement with the theoretical calculation. The Cu $3d$ states in β-brass are almost like the virtual bound states observed in dilute Cu alloys. The symmetric Lorentzian line shape of the Cu $3d$ peak in β-brass supports this observation.[29]

Although the spectral shapes are in good agreement with theory, the Cu $3d$ peak position in the experimental spectrum of β-brass is shifted by about 0.5 eV toward higher BE (Fig. 3). Also, for the calculated conduction band, the minimum (dip) appears at somewhat lower energy compared to the IPES spectrum (Fig. 2). To find a reason for this disagreement, the DOS was calculated with local-density approximation, but it was similar to that with GGA. Furthermore, the DOS calculated with optimized lattice constant a (=5.6144 a.u.) also remains unchanged. Nonstoichiometry changes the local environment and can shift the DOS peaks. However, previous XPS study for different Cu-Zn compositions show that the Cu $3d$ peak shifts to lower BE with decreasing Zn content,[12] which is in agreement with the trend that we observe between β- and α-brass. Here, the β-brass composition is $Cu_{0.6}Zn_{0.4}$, while the calculation is for CuZn. Thus, decreased Zn content in the actual sample would imply a shift of Cu $3d$ peak to lower BE compared to the calculated position for CuZn. In contrast, the experimental peak appears at higher BE with respect to the calculated peak. Thus, nonstoichiometry does not explain the shift. A possible reason for the disagreement could be related to the final-state effects in photoemission and inverse photoemission. For example, the final states of these two processes are $n-1$ and $n+1$ electron states, respectively, while the calculation is for n electron zero-temperature ground state. The final-state relaxation energy affects the BE,[30] and this is not considered by present theory.

Both IPES and XPS are highly surface sensitive techniques probing 10–20 Å of the surface.[29,30] Due to surface relaxation, the actual lattice constant at the surface might be different from the bulk CuZn that is used in the theory. In fact, contraction of the lattice constants for metallic surfaces and occurrence of oscillatory relaxation have been reported in literature.[31] So, we have performed the calculations by varying the lattice constant. Increase in a makes the agreement worse with the Cu $3d$ DOS shifting to lower BE and the dip in the unoccupied DOS shifts toward E_F. However, by decreasing a by 5% makes the agreement much better for both XPS and IPES. The Cu $3d$ peak shifts to higher BE by about 0.45 eV and also the FWHM increases by 0.2 eV compared to the Cu $3d$ valence band with uncontracted lattice constant (Fig. 3). Thus, both position and shape of calculated Cu $3d$ valence band are in better agreement with experiment. Furthermore, in the IPES spectrum, the dip shifts to higher energy by 0.7 eV resulting in improved concurrence with experiment (Fig. 2). Thus, possibility of about 5% lattice contraction at the surface is indicated by our study.

In conclusion, the electronic structure of α- and β-brass

has been studied by inverse photoemission spectroscopy and x-ray photoemission spectroscopy. The experimental data are interpreted with the aid of full potential calculations based on density-functional theory. The Cu 3*d* related peak in the valence band shifts to higher binding energy, becomes narrower and symmetric in β-brass compared to α-brass. The width of the primarily Cu 3*d* related unoccupied conduction band also narrows in β-brass. These observations can be related to the reduction of the overlap between Cu atoms due to change in structure and increase in Zn content. The spectral shape and the changes in the conduction and valence bands between α- and β-brass are in good agreement with the theoretical spectra. However, disagreement in the position of the DOS features in β-brass can possibly be ascribed to a lattice contraction at the surface. For CuZn (β-brass), the DOS exhibits a monotonic decrease across E_F with a dip at about 2 eV above E_F. Evidence of pseudogap at E_F is not observed for β-brass, although it is generally believed to be a Hume Rothery alloy.

P. Chaddah, V. C. Sahni, A. Gupta, S. M. Oak, and K. Horn are thanked for encouragement. Fundings from Max-Planck-D.S.T. Partner Group project and Ramanna Fellowship Research Grant are acknowledged.

*barman@csr.ernet.in

[1] P. E. A. Turchi, M. Sluiter, F. J. Pinski, D. D. Johnson, D. M. Nicholson, G. M. Stocks, and J. B. Staunton, Phys. Rev. Lett. **67**, 1779 (1991).
[2] D. A. Rowlands, J. B. Staunton, B. L. Györffy, E. Bruno, and B. Ginatempo, Phys. Rev. B **72**, 045101 (2005).
[3] F. Jona and P. M. Marcus, J. Phys.: Condens. Matter **13**, 5507 (2001).
[4] K. Tarafder, A. Chakrabarti, K. K. Saha, and A. Mookerjee, Phys. Rev. B **74**, 144204 (2006).
[5] R. Prasad, S. C. Papadopoulos, and A. Bansil, Phys. Rev. B **23**, 2607 (1981); R. S. Rao, R. Prasad, and A. Bansil, *ibid.* **28**, 5762 (1983); A. Bansil, H. Ehrenreich, L. Schwartz, and R. E. Watson, *ibid.* **9**, 445 (1974).
[6] V. L. Moruzzi, A. R. Williams, J. F. Janak, and C. Sofes, Phys. Rev. B **9**, 3316 (1974).
[7] H. L. Skriver and N. E. Christensen, Phys. Rev. B **8**, 3778 (1973).
[8] F. J. Arlinghaus, Phys. Rev. **157**, 491 (1967).
[9] H. Amar, K. H. Johnson, and C. B. Sommers, Phys. Rev. **153**, 655 (1967).
[10] M. M. Pant and S. K. Joshi, Phys. Rev. **184**, 635 (1969).
[11] D. Lewis, R. J. Cole, and P. Weightman, J. Phys.: Condens. Matter **11**, 8431 (1999).
[12] P. T. Andrews and L. A. Hisscott, J. Phys. F: Met. Phys. **5**, 1568 (1975).
[13] P. O. Nilsson and I. Lindau, J. Phys. F: Met. Phys. **1**, 854 (1971).
[14] J. S. Faulkner, Y. Wang, and G. M. Stocks, Phys. Rev. Lett. **81**, 1905 (1998).
[15] W. Hume-Rothery, J. Inst. Met. **35**, 295 (1926); H. Jones, Proc. Phys. Soc. London **49**, 250 (1937).
[16] V. F. Degtyareva, O. Degtyareva, M. K. Sakharov, N. I. Novokhatskaya, P. Dera, H. K. Mao, and R. J. Hemley, J. Phys.: Condens. Matter **17**, 7955 (2005).
[17] S. Banik, A. K. Shukla, and S. R. Barman, Rev. Sci. Instrum. **76**, 066102 (2005); A. K. Shukla, S. Banik, and S. R. Barman, Curr. Sci. **90**, 490 (2006).
[18] S. Banik, A. Chakrabarti, U. Kumar, P. K. Mukhopadhyay, A. M. Awasthi, R. Ranjan, J. Schneider, B. L. Ahuja, and S. R. Barman, Phys. Rev. B **74**, 085110 (2006); S. K. Pandey, A. Kumar, S. Banik, A. K. Shukla, S. R. Barman, and A. V. Pimpale, *ibid.* **77**, 113104 (2008).
[19] C. Biswas and S. R. Barman, Appl. Surf. Sci. **252**, 3380 (2006).
[20] S. R. Barman, S. Banik, and Aparna Chakrabarti, Phys. Rev. B **72**, 184410 (2005); S. R. Barman, S. Banik, A. K. Shukla, C. Kamal, and Aparna Chakrabarti, Europhys. Lett. **80**, 57002 (2007).
[21] R. J. Cole, N. J. Brooks, and P. Weightman, Phys. Rev. Lett. **78**, 3777 (1997).
[22] S. R. Barman and D. D. Sarma, Phys. Rev. B **51**, 4007 (1995).
[23] A. Chakrabarti, C. Biswas, S. Banik, R. S. Dhaka, A. K. Shukla, and S. R. Barman, Phys. Rev. B **72**, 073103 (2005).
[24] S. Gokhale, S. R. Barman, and D. D. Sarma, Phys. Rev. B **52**, 14526 (1995).
[25] J. P. Perdew, K. Burke, and M. Ernzerhof, Phys. Rev. Lett. **77**, 3865 (1996).
[26] P. Blaha, K. Schwartz, and J. Luitz, *WIEN97* (Karlheinz Schwarz, Technische Universität, Wien, Austria, 1999).
[27] A. K. Shukla, C. Biswas, R. S. Dhaka, S. C. Das, P. Krüger, and S. R. Barman, Phys. Rev. B **77**, 195103 (2008); G. Trambly de Laissardiére, D. N. Manh, and D. Mayou, Prog. Mater. Sci. **50**, 679 (2005).
[28] D. D. Sarma, N. Shanthi, S. R. Barman, N. Hamada, H. Sawada, and K. Terakura, Phys. Rev. Lett. **75**, 1126 (1995).
[29] S. Hüfner, *Photoelectron Spectroscopy*, 2nd ed. (Springer, Berlin, 1994).
[30] M. Cardona and L. Ley, *Photoemission in Solids: General Principles* (Springer-Verlag, Berlin, 1978).
[31] R. P. Gupta, Phys. Rev. B **23**, 6265 (1981); J. H. Cho, Ismail, Z. Zhang, and E. W. Plummer, *ibid.* **59**, 1677 (1999).